

Learning Environment-Aware Control Barrier Functions for Safe and Feasible Multi-Robot Navigation

Zhan Gao, Guang Yang and Amanda Prorok

Abstract— Control Barrier Functions (CBFs) have been applied to provide safety guarantees for robot navigation. Traditional approaches consider *fixed* CBFs during navigation and hand-tune the underlying parameters *a priori*. Such approaches are inefficient and vulnerable to changes in the environment. The goal of this paper is to learn CBFs for multi-robot navigation based on what robots perceive about their environment. In order to guarantee the feasibility of the navigation task, while ensuring robot safety, we pursue a trade-off between conservativeness and aggressiveness in robot behavior by defining dynamic *environment-aware* CBF constraints. Since the explicit relationship between CBF constraints and navigation performance is challenging to model, we leverage reinforcement learning to learn time-varying CBFs in a model-free manner. We parameterize the CBF policy with graph neural networks (GNNs), and design GNNs that are translation invariant and permutation equivariant, to synthesize decentralized policies that generalize across environments. The proposed approach maintains safety guarantees (due to the underlying CBFs), while optimizing navigation performance (due to the reward-based learning). We perform simulations that compare the proposed approach with fixed CBFs tuned by exhaustive grid-search. The results show that environment-aware CBFs are capable of adapting to robot movements and obstacle changes, yielding improved navigation performance and robust generalization.

I. INTRODUCTION

Multi-robot systems have attracted increasing attention for spatially distributed tasks, among which safe and efficient motion planning is one of the central problems [1]–[3]. In the context of multi-robot navigation, model-based approaches often assume full accessibility to the environment and system dynamics, and require designing explicit objective functions and well-tuned hyper-parameters prior to robots’ deployments. On the other hand, data-driven approaches often do not provide proven safety guarantees, and system behaviors are difficult to explain. In this paper, we focus on finding a middle-ground that is capable of leveraging the advantages from both approaches.

The problem of providing multi-robot navigation with convergence to labeled destinations and ensurance of safety constraints can be mapped to a sequence of real-time optimization problems by using Control Barrier Functions (CBFs) and Control Lyapunov Functions (CLFs), where the former allows the robots to move safely without collision and the latter guides the robots towards target states. The combination of CBF and CLF based methods have been widely used for safety-critical controls [4], [5]. While providing safety guarantees, traditional CBF-based approaches require

Zhan Gao, Guang Yang and Amanda Prorok are with Department of Computer Science and Technology, University of Cambridge, CB3 0FD (email: zg292@cam.ac.uk; gy268@cam.ac.uk; asp45@cam.ac.uk)

This work was supported by European Research Council (ERC) Project 949940 (gAla).

manually setting CBF parameters within CBF constraints [4]–[7]. This could plan overly conservative trajectories with strong CBF constraints or overly aggressive trajectories with relaxed ones, both of which could lead to infeasible solutions, i.e., no admissible control is available to steer the robots to their destinations. Moreover, such issues occur more frequently when the environment becomes cluttered with moving robots and an increasing number of obstacles, as the number of CBF constraints scales with that of the robots and obstacles. Many existing works preset CBF parameters before deployment and fix the latter throughout the navigation procedure. This requires re-tuning CBF parameters as the environment changes. In the absence of online re-tuning, the multi-robot system is vulnerable to dynamic environments where robot configurations differ across time. We are, hence, interested in developing a model that captures time-varying information and tunes CBF parameters in real time.

Instead of hand-tuning and fixing CBF parameters at the outset, we propose a methodology that tunes the latter based on robot and obstacle states in a real-time manner. The goal is to find an optimal sequence of time-varying CBF parameters for robots that balances conservativeness and aggressiveness of CBF constraints, to optimize navigation performance. Due to the challenge of explicitly modeling the relationship between CBF parameters and navigation performance, we parameterize the CBF-tuning policy with graph neural networks (GNNs) and learn the latter with model-free reinforcement learning (RL). Due to the distributed nature of GNNs [8]–[11], the resulting policy allows for a decentralized implementation, i.e., it can be executed on each robot locally with only neighborhood information, yielding an efficient and scalable solution for multi-robot systems.

Related work. There are two groups of common CBF based techniques in multi-robot control: model-based [12]–[15] and data-driven approaches [16]–[18]. The classic model-based CBF framework requires full knowledge of the environment and the CBF parameters are fixed for all time. The CBF constraints are affine in the control variable that can be used to formulate a quadratic programming (QP) based controller. The QP controller can be either paired with CLF to ensure state convergence, or used to track a reference control. This framework provides safety guarantees for multi-robot control. By contrast, the data-driven approaches directly approximate CBFs with neural networks. However, these approaches sacrifice safety guarantees in the process. The work in [19] combined model-based and data-driven approaches by learning a backup CBF constraint to enhance the safety guarantee. In terms of the feasibility of CBF-QP controller, [20] designed a feasibility guaranteed controller for traffic merging problems. The work in [21] studied

the feasibility of a CBF-based model predictive controller (MPC) in a discrete time setting, while [22] introduced a decaying term paired with CBFs to improve the feasibility of the MPC controller. Moreover, [23] extended the class \mathcal{K} function of CBFs for forward invariance in continuous time. However, *none of the aforementioned works update the CBF parameters based on changes in the the robot's perceived environment*. A more closely related work [24] introduces a framework to find optimal CBF parameters that minimize the control efforts over a given time horizon. It uses an SVM classifier to filter out CBF parameters that cause the QP controller to be infeasible, to reduce the search space of optimal CBF parameters. However, it assumes fixed CBF constraints during navigation and does not address multi-robot scenarios.

Contributions. Our contributions are as follows:

- 1) We propose a novel safety-critical framework that adapts CBF constraints to time-varying environments using a data-driven approach for multi-robot navigation. It inherits safety guarantees from traditional CBF constraints and improves navigation performance due to real-time CBF tuning.
- 2) We parameterize the CBF-tuning policy with GNNs, which allows for a decentralized implementation, and conduct training with model-free RL, which overcomes the challenge of explicitly modeling the relationship between CBF parameters and navigation performance. Moreover, the proposed GNN is translation invariant and permutation equivariant, improving the policy's robustness to unknown environment changes.
- 3) We validate the proposed framework with various environment configurations. The results show the proposed framework can generalize to different map configurations and outperforms the existing approach with fixed CBF parameters that are tuned apriori through exhaustive grid-search.

II. PRELIMINARIES

In this section, we introduce preliminaries about system dynamics, CLFs for destination convergence, and CBFs for safety guarantees in multi-robot navigation.

System dynamics Consider a multi-robot system with N robots $\mathcal{A} = \{A_i\}_{i=1}^N$ in a 2-D environment with M obstacles $\{O_j\}_{j=1}^M$. The robot dynamics take the form of

$$\dot{\mathbf{x}}_i = f(\mathbf{x}_i) + g(\mathbf{x}_i)\mathbf{u}_i, \quad (1)$$

where $\mathbf{x}_i \in \mathbb{R}^n$ is the internal state, $\mathbf{u}_i \in \mathbb{R}^m$ is the control input of the i -th robot and $\dot{\mathbf{x}}_i$ is the derivative of \mathbf{x}_i w.r.t. time t for $i = 1, \dots, N$. The flow vectors $f(\mathbf{x}_i)$, $g(\mathbf{x}_i)$ are locally Lipschitz continuous. The obstacles are static and distributed in the environment. The robots have a sensing range $\sigma \in \mathbb{R}^+$ that only provides them with partial observability of the entire environment, i.e., each robot A_i can obtain the states of the other robots $\{\mathbf{x}_j\}_{j \in \mathcal{N}_i}$ and the positions of the obstacles $\{\mathbf{p}_{k,o}\}_{k \in \mathcal{N}_i}$ within the neighborhood of radius σ where \mathcal{N}_i is the neighbor set for $i = 1, \dots, N$ – see Fig. 1. We consider *decentralized* control policies as

$$\pi_i(\mathbf{u}_i | \mathbf{x}_i, \{\mathbf{x}_j\}_{j \in \mathcal{N}_i}, \{\mathbf{p}_{k,o}\}_{k \in \mathcal{N}_i}), \text{ for } i = 1, \dots, N \quad (2)$$

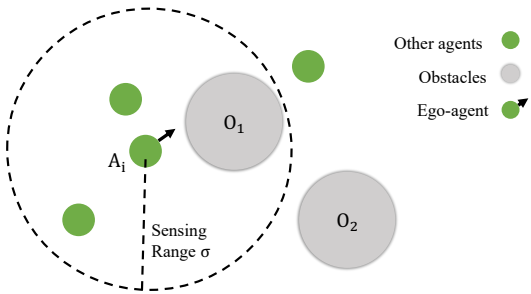


Fig. 1. Each robot A_i only communicates / senses the other robots and obstacles within its sensing range σ (marked with the dashed circle). In this example, there are two CBF constraints w.r.t. the other robots and one CBF constraint w.r.t. obstacle O_1 , which results in a total of three CBF constraints for ego-robot A_i .

that drive the robots from initial states $\mathbf{X}^{(0)} := \{\mathbf{x}_i^{(0)}\}_{i=1}^N$ to target states $\mathbf{X}^d := \{\mathbf{x}_i^d\}_{i=1}^N$ with local neighborhood information while avoiding collisions.

Control Lyapunov function (CLF). The CLF is designed to encode the goal reaching requirement, i.e., the saistification of CLF constraints guarantees robots converging to their destinations. We define the exponentially-stabilizing CLF in the following, which ensures that the robot converges to its destination under an exponentially decaying bound [25].

Definition 1: Given the system (1), for each robot A_i , a positive definite function $V_i(\mathbf{x}_i) : \mathbb{R}^n \mapsto \mathbb{R}$ is an exponentially-stabilizing control Lyapunov function (ES-CLF) [25] if there exists a positive constant $\epsilon \geq 0$, such that

$$\inf_{\mathbf{u}_i \in \mathbb{U}_i} [\mathcal{L}_f V_i(\mathbf{x}_i) + \mathcal{L}_g V_i(\mathbf{x}_i) u_i + \epsilon V_i(\mathbf{x}_i)] \leq 0, \text{ for } \mathbf{x}_i \in \mathbb{R}^n, \quad (3)$$

where $\mathcal{L}_f V_i(\mathbf{x}_i)$ is the Lie derivative [26] of the continuously differentiable function $V_i(\mathbf{x}_i)$ along the dynamics $f(\mathbf{x}_i)$, defined as $\mathcal{L}_f V_i(\mathbf{x}_i) := \frac{\partial V_i(\mathbf{x}_i)}{\partial \mathbf{x}_i} f(\mathbf{x}_i)$, and \mathbb{U}_i is the control space of robot A_i .

The Lyapunov function $V_i(\mathbf{x}_i)$ is positive definite with a minimum value of zero, and robot A_i reaches its destination when $V_i(\mathbf{x}_i) = 0$. By enforcing (3), $V_i(\mathbf{x}_i)$ decreases at a rate of ϵ and guarantees the robot converging to its destination, where ϵ controls the convergence rate of state trajectory.

Control barrier function (CBF). The CBF is designed to avoid static obstacles, as well as to prevent inter-collisions among moving robots. In this paper, we consider higher-order control barrier functions (HOCBFs) to ensure *forward invariance* of the state trajectory [27], i.e., if the system (1) starts within safety sets (6), it will always stay within the safety sets. To proceed, we introduce the concept of relative degree. For each robot A_i , given a continuous function over state $h_i(\mathbf{x}_i) : \mathbb{R}^n \mapsto \mathbb{R}$, the r_b -th derivative of $h_i(\mathbf{x}_i)$ w.r.t. time t of the robot dynamics (1) can be computed as

$$h_i^{r_b}(\mathbf{x}_i) = \mathcal{L}_f^{r_b} h_i(\mathbf{x}_i) + \mathcal{L}_g^{r_b} \mathcal{L}_f^{r_b-1} h_i(\mathbf{x}_i) \mathbf{u}_i, \quad (4)$$

where $\mathcal{L}_f^r h_i(\mathbf{x}_i) := \frac{\partial \mathcal{L}_f^{r-1} h_i(\mathbf{x}_i)}{\partial \mathbf{x}_i} f(\mathbf{x}_i)$, $\mathcal{L}_g^r \mathcal{L}_f^{r-1} h_i(\mathbf{x}_i) := \frac{\partial \mathcal{L}_f^{r-1} h_i(\mathbf{x}_i)}{\partial \mathbf{x}_i} g(\mathbf{x}_i)$ are higher-order Lie derivatives [26]. The *relative degree* $r_b \geq 0$ is defined as the smallest natural number such that $\mathcal{L}_g \mathcal{L}_f^{r_b-1} h_i(\mathbf{x}_i) \mathbf{u}_i \neq 0$. It is the least number

of derivatives needed for $h_i(\mathbf{x}_i)$ to make the control input \mathbf{u}_i show up [cf. (4)], such that we can enforce constraints on \mathbf{u}_i for safety guarantees. Then, we define a series of functions $\{\Psi_{i,r}\}_{r=0}^{r_b}$ based on $h_i(\mathbf{x}_i)$ as

$$\begin{aligned}\Psi_{i,0}(\mathbf{x}_i) &= h_i(\mathbf{x}_i), \\ \dots \\ \Psi_{i,r_b}(\mathbf{x}_i) &= \dot{\Psi}_{i,r_b-1} + \alpha_{i,r_b}(\Psi_{i,r_b-1}(\mathbf{x}_i)),\end{aligned}\tag{5}$$

where $\alpha_{i,r} : [0, a) \mapsto [0, \infty)$ for some $a > 0$ is strictly increasing, referred to as a class \mathcal{K} function for robot A_i [26]. Next, we define a series of super-level sets $\{\mathcal{C}_{i,r}\}_{r=0}^{r_b}$ as

$$\begin{aligned}\mathcal{C}_{i,0} &= \{\mathbf{x}_i \in \mathbb{R}^n \mid \Psi_{i,0}(\mathbf{x}_i) \geq 0\}, \\ \dots \\ \mathcal{C}_{i,r_b} &= \{\mathbf{x}_i \in \mathbb{R}^n \mid \Psi_{i,r_b}(\mathbf{x}_i) \geq 0\}.\end{aligned}\tag{6}$$

With these concepts, the HOCBF is defined as follows.

Definition 2: [27] Given the safety sets (6) and the corresponding functions (5), the r_b -th order differentiable function $h_i : \mathbb{R}^n \mapsto \mathbb{R}$ is a HOCBF for system (1) if there exist functions $\alpha_{i,1}, \dots, \alpha_{i,r_b}$ such that

$$\Psi_{i,r_b}(\mathbf{x}_i) \geq 0\tag{7}$$

for all $\mathbf{x}_i \in \mathcal{C}_{i,0} \cap \dots \cap \mathcal{C}_{i,r_b}$. The system is forward invariant [28] and the system trajectory remains safe for all time.

III. PROBLEM FORMULATION

In this section, we start by formulating the multi-robot navigation problem based on CBFs and CLFs, and proceed to proposing the problem of environment-aware CBF optimization. Specifically, assume the robots and obstacles are disk-shaped with radii $\{R_i\}_{i=1}^N$ and $\{R_k\}_{k=1}^M$, respectively. Let $\{\mathbf{p}_i\}_{i=1}^N$, $\{\mathbf{v}_i\}_{i=1}^N$ and $\{\mathbf{d}_i\}_{i=1}^N$ be the positions, velocities and destinations of the robots \mathcal{A} , which are determined by the internal states $\{\mathbf{x}_i\}_{i=1}^N$, and $\{\mathbf{p}_{k,o}\}_{k=1}^M$ be the positions of the obstacles. The goal of multi-robot navigation is to move robots towards their destinations while avoiding collision. The destination convergence is equivalent to the state convergence as $\lim_{t \rightarrow T} \mathbf{x}_i^{(t)} = \mathbf{x}_i^d$ with T the maximal time step for $i = 1, \dots, N$. The collision avoidance is equivalent to the safety constraints on the robot states, i.e.,

$$\mathcal{C}_{i,a}^{(t)} = \{\mathbf{x}_i^{(t)} \in \mathbb{R}^n \mid \|\mathbf{p}_i^{(t)} - \mathbf{p}_j^{(t)}\| \geq \frac{R_i + R_j}{2}, j \neq i\},\tag{8}$$

$$\mathcal{C}_{i,o}^{(t)} = \{\mathbf{x}_i^{(t)} \in \mathbb{R}^n \mid \|\mathbf{p}_i^{(t)} - \mathbf{p}_{k,o}^{(t)}\| \geq \frac{R_i + R_k}{2}, k = 1, \dots, M\},\tag{9}$$

where $\|\cdot\|$ is the vector norm. With these in place, we formulate the multi-robot navigation problem as follows.

Problem 1 (Safe and feasible multi-robot navigation): Given the multi-robot system \mathcal{A} with system dynamics (1), the initial states $\{\mathbf{x}_i^{(0)}\}_{i=1}^N$ and the target states $\{\mathbf{x}_i^d\}_{i=1}^N$ satisfying $\{f(\mathbf{x}_i^d) = 0\}_{i=1}^N$, find decentralized policies $\{\pi_i : \mathbb{R}^{|\mathcal{N}_i| \times n} \rightarrow \mathbb{R}^m\}_{i=1}^N$ that generate the control inputs such that

$$\lim_{t \rightarrow T} \|\mathbf{x}_i^{(t)} - \mathbf{x}_i^d\| = 0,\tag{10}$$

$$\text{s.t. } \mathbf{x}_i^{(t)} \in \mathcal{C}_{i,a}^{(t)} \cap \mathcal{C}_{i,o}^{(t)}\tag{11}$$

for $i = 1, \dots, N$.

The first condition (10) guarantees the state convergence, i.e., the navigation, and the second condition (11) guarantees the state safety, i.e., the collision avoidance. Problem 1 is challenging because (i) the control policies are decentralized and generate control inputs based on only local neighborhood information, (ii) the safety sets in (8)-(9) can be either convex or non-convex, and (iii) the safety sets are time-varying and depend on moving robots.

We propose to solve the decentralized multi-robot navigation problem with a CBF-CLF based quadratic programming (QP) controller. Specifically, at each time step t , we can formulate an associated QP problem as

$$\begin{aligned}\min_{\mathbf{u}_i^{(t)} \in \mathbb{U}_i, \delta_i^{(t)} \in \mathbb{R}} \quad & \|\mathbf{u}_i^{(t)}\|_2 + \xi(\delta_i^{(t)})^2 \\ \text{s.t. } \quad & \mathcal{L}_f^{r_b} h_{i,l}(\mathbf{x}_i^{(t)}) + \mathcal{L}_g \mathcal{L}_f^{r_b-1} h_{i,l}(\mathbf{x}_i^{(t)}) \mathbf{u}_i^{(t)} + \alpha_{i,r_b}(h_{i,l}(\mathbf{x}_i^{(t)})) \geq 0, \\ & \text{for all } l = 0, \dots, N_{i,\text{CBF}}, \\ & \mathcal{L}_f V_i(\mathbf{x}_i^{(t)}) + \mathcal{L}_g V_i(\mathbf{x}_i^{(t)}) \mathbf{u}_i^{(t)} + \epsilon V_i(\mathbf{x}_i^{(t)}) + \delta_i^{(t)} \leq 0, \\ & \mathbf{x}_i^{(t)} \in \text{Int}(\mathcal{C}_i^{(t)}), \text{ for all } i = 1, \dots, N,\end{aligned}\tag{12}$$

where $\xi \in \mathbb{R}^+$ is a penalty weight for slack variable $\delta_i \in \mathbb{R}$ that is selected based on how strictly the CLF needs to be enforced, $\text{Int}(\mathcal{C}_i^{(t)})$ the interior of the safety sets in (8)-(9), and $N_{i,\text{CBF}}$ the number of CBF constraints based on robot A_i 's perceived robots and obstacles. For example, there are two CBF constraints w.r.t. the other robots and one w.r.t. the obstacle in Fig. 1. The control input is bounded by $\mathbf{u}_i^{(t)} \in \mathbb{U}_i$ given the robot's physical constraints. The QP is solved per time step to generate $\mathbf{u}_i^{(t)}$ until the destination is reached. The selection of the class \mathcal{K} function $\alpha_{i,r_b}(\cdot)$ determines how strictly we want to enforce safety, and therefore will change the behavior of the robot to be either conservative or aggressive.

While the QP controller guarantees safety and convergence, it may be infeasible, i.e., there is no solution for (12), at some time step, resulting in the failure of the multi-robot navigation task. Specifically, given system dynamics (1), CBF constraints (19), and CLF constraints (3) at each time step we define the super-level set that satisfies the constraints in the QP (12) for robot A_i as

$$\mathbb{U}_{i,\text{CBF,CLF}}^{(t)} := \left\{ \mathbf{u}_i^{(t)} \in \mathbb{R}^m \mid \begin{array}{l} \mathcal{L}_g h_{i,l}(\mathbf{x}_i^{(t)}) \mathbf{u}_i^{(t)} \geq -\mathcal{L}_f h_{i,l}(\mathbf{x}_i^{(t)}), \\ -\alpha_{i,r_b}(h_{i,l}(\mathbf{x}_i^{(t)})), \text{ for all } l, \\ -\mathcal{L}_g V_i(\mathbf{x}_i^{(t)}) \mathbf{u}_i^{(t)} \geq \mathcal{L}_f V_i(\mathbf{x}_i^{(t)}), \\ +\epsilon V_i(\mathbf{x}_i^{(t)}) + \delta_i^{(t)} \end{array} \right\}.\tag{13}$$

With the control space \mathbb{U}_i , we define feasibility of (12) as

$$\mathbb{U}_i \cap \mathbb{U}_{i,\text{CBF,CLF}}^{(t)} \neq \emptyset.\tag{14}$$

For conservative CBFs, the resulting constraints are strict and there may be no feasible solution for $\mathbb{U}_{i,\text{CBF,CLF}}^{(t)}$, i.e., $\mathbb{U}_{i,\text{CBF,CLF}}^{(t)} = \emptyset$. For aggressive CBFs, the resulting constraints are relaxed and the robots may be too close to the obstacles or each other, such that the QP controller generates some control input that is beyond the robot's capacity

\mathbb{U}_i . Both scenarios lead to the infeasibility of (14), which indicates an explicit trade-off inherent in CBF constraints.

The aforementioned issue makes hand-tuning CBF constraints difficult when the environment becomes cluttered with increasing numbers of robots and obstacles. Moreover, fixed CBF constraints may not work well for the dynamic environment with moving robots and well-tuned CBF constraints could suffer from performance degradation with environment changes. In this work, we propose to conduct real-time adjustments of CBF constraints that adapt to the perceived dynamic environment during the multi-robot navigation, pursuing a trade-off between robots' conservative and aggressive behavior. We refer to the latter as *environment-aware CBFs*. Specifically, we define decentralized CBF-tuning policies as

$$\pi_{i,\text{CBF}}\left(\alpha_{i,r_b} \mid \mathbf{x}_i, \{\mathbf{x}_j\}_{j \in \mathcal{N}_i}, \{\mathbf{p}_{k,o}\}_{k \in \mathcal{N}_i}\right), i = 1, \dots, N \quad (15)$$

which generates the class \mathcal{K} function α_{i,r_b} , i.e., the CBF constraints, based on local neighborhood information. At each time step t , a new class \mathcal{K} function $\alpha_{i,r_b}^{(t)}$ is generated for each robot A_i and passed into CBF constraints for solving (12) to generate the control input. Given the objective function $f(\{\pi_{i,\text{CBF}}\}_{i=1}^N, \mathbf{X}^{(0)}, \mathbf{X}^d)$ that depends on CBF-tuning policies $\{\pi_{i,\text{CBF}}\}_{i=1}^N$, the initial robot states $\mathbf{X}^{(0)}$ and the target states \mathbf{X}^d , we can formulate the problem of environment-aware CBF optimization in the following.

Problem 2 (Environment-aware CBF optimization):

Given the multi-robot navigation with initial states $\mathbf{X}^{(0)}$ and target states \mathbf{X}^d , find CBF-tuning policies $\{\pi_{i,\text{CBF}}\}_{i=1}^N$ that generate environment-aware CBF constraints to maximize the objective function $f(\{\pi_{i,\text{CBF}}\}_{i=1}^N, \mathbf{X}^{(0)}, \mathbf{X}^d)$, i.e., the navigation performance, and guarantee the feasibility of QP controller [cf. (14)].

IV. METHODOLOGY

In this section, we specify the decentralized CLF-CBF based QP controller to solve the problem of multi-robot navigation and leverage model-free reinforcement learning with decentralized GNNs to solve the problem of CBF optimization. We consider a linear system for each robot A_i , which has the following system dynamics

$$\begin{bmatrix} \dot{p}_{i,1} \\ \dot{p}_{i,2} \end{bmatrix} = \begin{bmatrix} 0 & 0 \\ 0 & 0 \end{bmatrix} \begin{bmatrix} p_{i,1} \\ p_{i,2} \end{bmatrix} + \begin{bmatrix} 1 & 0 \\ 0 & 1 \end{bmatrix} \begin{bmatrix} u_{i,1} \\ u_{i,2} \end{bmatrix}, \quad (16)$$

where $\mathbf{p}_i = [p_{i,1}, p_{i,2}]^\top$ is the position and $\mathbf{u}_i = [u_{i,1}, u_{i,2}]^\top$ the control input of robot A_i for $i = 1, \dots, N$.

A. CLF-CBF-QP Controller

Given the destination $\mathbf{d}_i = [d_{i,1}, d_{i,2}]^\top$ of robot A_i , define a Lyapunov function candidate as

$$V_i(\mathbf{x}) = (p_{i,1} - d_{i,1})^2 + (p_{i,2} - d_{i,2})^2 \quad (17)$$

and the CLF constraint as

$$\mu_i := 2(\mathbf{p}_i - \mathbf{p}_i^d)^\top \mathbf{u}_i + \epsilon V_i(\mathbf{x}_i) + \delta_i \leq 0. \quad (18)$$

for $i = 1, \dots, N$. Since the *relative degree* of the linear system is 1 [cf. (16)], define the CBF constraint as

$$\Psi_{i,1}(\mathbf{x}_i) = \dot{\Psi}_{i,0} + \zeta \Psi_{i,0}(\mathbf{x}_i)^\eta, \quad (19)$$

where $\Psi_{i,0} = h_i(\mathbf{x}_i)$ and the class \mathcal{K} function $\alpha_{i,1}(h_i(\mathbf{x}_i)) = \zeta h_i(\mathbf{x}_i)^\eta$ is specified by the CBF parameters $\zeta \in \mathbb{R}^+$ and $\eta \in \mathbb{R}^+$. With safety conditions (8) and (9), define the safety sets as

$$\begin{aligned} h_{i,j,a}(\mathbf{x}_i) &= (p_{i,1} - p_{j,1})^2 + (p_{i,2} - p_{j,2})^2 - (R_i + R_j)^2, \quad (20) \\ h_{i,k,o}(\mathbf{x}_i) &= (p_{i,1} - p_{k,1,o})^2 + (p_{i,2} - p_{k,2,o})^2 - (R_i + R_k)^2, \end{aligned}$$

where $h_{i,j,a}$ is the safety set for avoiding collision between the robots A_i and A_j , and $h_{i,k,o}$ is the safety set for avoiding collision between robot A_i and obstacle O_k with $\mathbf{p}_{k,o} = [p_{k,1,o}, p_{k,2,o}]^\top$ the position of obstacle k . The resulting CBF candidates that are affine w.r.t. the control input $\mathbf{u}_i = [u_{i,1}, u_{i,2}]^\top$ are

$$\begin{aligned} \nu_{i,j,a} &:= 2(\mathbf{p}_i - \mathbf{p}_j)^\top \mathbf{u}_i - 2(\mathbf{p}_i - \mathbf{p}_j)^\top \mathbf{v}_j + \zeta_{i,a} h_{i,j,a}^{\eta_{i,a}} \geq 0, \\ \nu_{i,k,o} &:= 2(\mathbf{p}_i - \mathbf{p}_k)^\top \mathbf{u}_i + \zeta_{i,o} h_{i,k,o}^{\eta_{i,o}} \geq 0, \end{aligned} \quad (21)$$

where $\zeta_{i,a}, \eta_{i,a}$ are CBF parameters of robot A_i w.r.t. the other robots and $\zeta_{i,o}, \eta_{i,o}$ are CBF parameters of robot A_i w.r.t. the obstacles, and $h_{i,j,a}, h_{i,k,o}$ are concise notations of $h_{i,j,a}(\mathbf{x}_i), h_{i,k,o}(\mathbf{x}_i)$. In this context, each robot has two sets of CBF parameters for the other robots and for the obstacles, respectively. We can then formulate the QP controller at each time step t as

$$\begin{aligned} \min_{\mathbf{u}_i^{(t)} \in \mathbb{U}_i, \delta_i^{(t)} \in \mathbb{R}} \quad & \|\mathbf{u}_i^{(t)}\|_2 + \xi(\delta_i^{(t)})^2 \\ \text{s.t.} \quad & \nu_{i,j,a}(h_{i,j,a}(\mathbf{x}_i^{(t)}), \mathbf{u}_i^{(t)}) \geq 0, \text{ for all } j \in \mathcal{N}_i, \\ & \nu_{i,k,o}(h_{i,k,o}(\mathbf{x}_i^{(t)}), \mathbf{u}_i^{(t)}) \geq 0, \text{ for all } k \in \mathcal{N}_i, \\ & \mu_i(V_i(\mathbf{x}_i^{(t)}), \mathbf{u}_i^{(t)}, \delta_i^{(t)}) \leq 0, \\ & \mathbf{x}_i^{(t)} \in \text{Int}(\mathcal{C}_i^{(t)}) \end{aligned} \quad (22)$$

for $i = 1, \dots, N$. The QP controller generates the control input $\mathbf{u}_i^{(t)}$ for robot A_i at each time step t towards its target state in a decentralized manner.

B. Reinforcement Learning

As the class \mathcal{K} function α_{i,r_b} of CBF constraints are determined by the CBF parameters $\zeta_{i,a}, \eta_{i,a}$ for the other robots and $\zeta_{i,o}, \eta_{i,o}$ for the obstacles at robot A_i , respectively, learning the CBF constraints is equivalent to learning the CBF parameters $\zeta_i = [\zeta_{i,a}, \zeta_{i,o}]^\top, \eta_i = [\eta_{i,a}, \eta_{i,o}]^\top$ at each robot A_i for $i = 1, \dots, N$. Since it is challenging to explicitly model the relationship between the CBF parameters and the navigation performance, we formulate the CBF optimization problem in the RL domain and learn the CBF-tuning policy in a model-free manner.

We start by defining a partially observable Markov decision process. At each time t , the robots are defined by states $\mathbf{X}^{(t)} = [\mathbf{x}_1^{(t)}, \dots, \mathbf{x}_N^{(t)}]$. Each robot A_i observes its local state $\mathbf{x}_i^{(t)}$, communicates with its neighboring robots, and senses its neighboring obstacles to collect the neighborhood information $\{\mathbf{x}_j^{(t)}\}_{j \in \mathcal{N}_i}$ and $\{\mathbf{p}_{k,o}\}_{k \in \mathcal{N}_i}$. The CBF-tuning policy $\pi_{i,\text{CBF}}(\mathbf{x}_i^{(t)}, \{\mathbf{x}_j^{(t)}\}_{j \in \mathcal{N}_i}, \{\mathbf{p}_{k,o}\}_{k \in \mathcal{N}_i})$ generates the CBF parameters $\zeta_i^{(t)}$ and $\eta_i^{(t)}$, which is a distribution over ζ_i and η_i conditioned on $\mathbf{x}_i^{(t)}, \{\mathbf{x}_j^{(t)}\}_{j \in \mathcal{N}_i}$ and $\{\mathbf{p}_{k,o}\}_{k \in \mathcal{N}_i}$. The CBF parameters $\zeta_i^{(t)}, \eta_i^{(t)}$ are fed into the QP controller

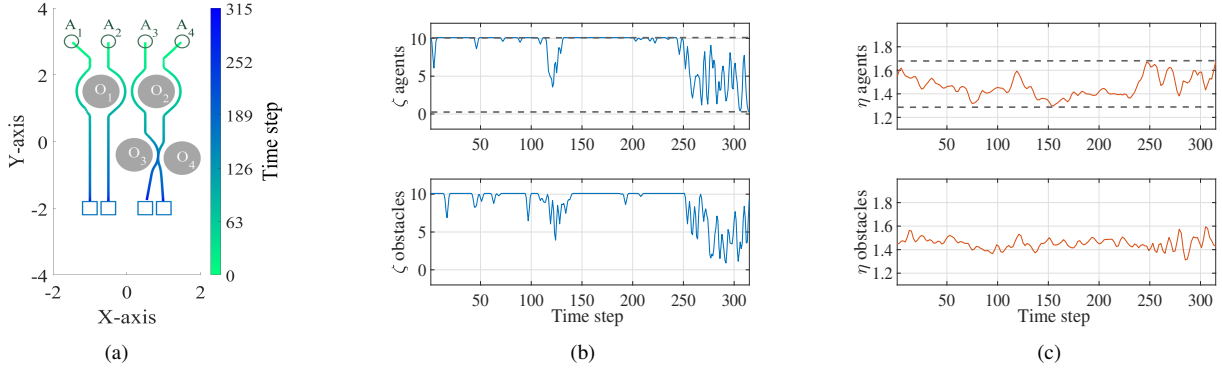


Fig. 2. (a) Robot trajectories with time-varying CBF parameters generated by GNN-based policy. Green circles are initial positions, blue squares are goal positions, and grey circles are obstacles. Green-to-blue lines are trajectories of robots and the color bar represents the time scale. (b) Time-varying CBF parameters $\zeta_{3,a}$ and $\eta_{3,a}$ of robot A_3 that accounts for collision avoidance to the other robots. (c) Time varying CBF parameters $\zeta_{3,o}$ and $\eta_{3,o}$ of robot A_3 that accounts for collision avoidance to the obstacles. The vertical lines in the top plots of (b) and (c) represent the maximal and minimal values of time-varying CBF parameters generated by GNN-based policy.

(22), and the latter generates the control action $\mathbf{u}_i^{(t)}$ that drives the local state from $\mathbf{x}_i^{(t)}$ to $\mathbf{x}_i^{(t+1)}$ based on the robot's dynamics (16) for $i = 1, \dots, N$. The reward function $r_i(\mathbf{X}^{(t)})$ represents the instantaneous navigation performance of robot A_i at time t , which consists of two components: (i) the navigation reward $r_{i,\text{nav}}$ and (ii) the QP's feasibility reward $r_{i,\text{infs}}$, i.e.,

$$r_i^{(t)} = r_{i,\text{nav}}^{(t)} + \beta_i r_{i,\text{infs}}^{(t)} \quad (23)$$

for $i = 1, \dots, N$, where $r_i^{(t)}, r_{i,\text{nav}}^{(t)}, r_{i,\text{infs}}^{(t)}$ are concise notations of $r_i(\mathbf{X}^{(t)}), r_{i,\text{nav}}(\mathbf{X}^{(t)}), r_{i,\text{infs}}(\mathbf{X}^{(t)})$ and β_i is the regularization parameter. The first term in (23) represents the task-relevant performance of robot A_i , while the second term in (23) corresponds to the feasibility of the QP controller with the generated CBF parameters, e.g., it penalizes the scenario where the resulting QP controller has no feasible solution with overly conservative or aggressive CBF parameters. The total reward of the multi-robot system is defined as $r^{(t)} = \sum_{i=1}^N r_i^{(t)}$. With the discount factor γ that accounts for the future rewards, the expected discounted reward can be represented as

$$R(\mathbf{X}^{(0)}, \mathbf{X}^d, \{\mathbf{p}_{k,o}\}_{k=1}^M | \{\pi_{i,\text{CBF}}\}_{i=1}^N) = \mathbb{E} \left[\sum_{t=0}^{\infty} \gamma^t r^{(t)} \right] = \sum_{i=1}^N \mathbb{E} \left[\sum_{t=0}^{\infty} \gamma^t r_{i,\text{nav}}^{(t)} \right] + \sum_{i=1}^N \beta_i \mathbb{E} \left[\sum_{t=0}^{\infty} \gamma^t r_{i,\text{infs}}^{(t)} \right], \quad (24)$$

where the expectation $\mathbb{E}[\cdot]$ is with respect to the CBF-tuning policy. The expected discounted reward in (24) corresponds to the objective function in the CBF optimization problem 2, which transforms the latter into the RL domain. By parameterizing the policies $\{\pi_{i,\text{CBF}}\}_{i=1}^N$ with information processing architectures $\{\Phi_i(\mathbf{x}_i^{(t)}, \{\mathbf{x}_j^{(t)}\}_{j \in \mathcal{N}_i}, \{\mathbf{p}_{k,o}\}_{k \in \mathcal{N}_i}, \boldsymbol{\theta}_i)\}_{i=1}^N$ of parameters $\{\boldsymbol{\theta}_i\}_{i=1}^N$, the goal is to learn optimal parameters $\{\boldsymbol{\theta}_i^*\}_{i=1}^N$ that maximize the expected discounted reward $R(\mathbf{X}^{(0)}, \mathbf{X}^d, \{\mathbf{p}_{k,o}\}_{k=1}^M | \{\boldsymbol{\theta}_i\}_{i=1}^N)$. We solve the latter by updating $\{\boldsymbol{\theta}_i\}_{i=1}^N$ through policy gradient ascent.

C. Graph Neural Networks

We propose to parameterize the CBF-tuning policy with GNNs [29]–[31], and design a GNN architecture that not

only allows for a decentralized implementation but also translation invariance and permutation equivariance. The former makes each robot capable of generating CBF parameters with partially observed states, while the latter facilitates robust transfer to unseen scenarios and improves sample efficiency for training.

The multi-robot system can be modeled as a graph $\mathcal{G} = \{\mathcal{V}, \mathcal{E}\}$ with the node set $\mathcal{V} = \{A_1, \dots, A_N\}$ representing the robots and the edge set \mathcal{E} representing communication links between neighboring robots. The graph structure can be captured by an adjacency matrix \mathbf{A} , where $[\mathbf{A}]_{ij} \neq 0$ if and only if there exists an edge between the nodes A_i and A_j . The graph signal \mathbf{X} captures the node states, which is a matrix with the i th column $[\mathbf{X}]_i = \mathbf{x}_i$ associated to the state of node A_i . In the context of multi-robot control, we consider the state of node A_i as the position \mathbf{p}_i , velocity \mathbf{v}_i and destination \mathbf{d}_i of robot A_i for $i = 1, \dots, N$.

Motivated by the observation that CBFs and CLFs need only relative information (e.g., relative positions between robots and obstacles) [cf. (17)–(20)], we design a GNN that leverages relative information to generate CBF parameters. For each node A_i with the state \mathbf{x}_i , it can obtain the states of the neighboring nodes $\{\mathbf{x}_j\}_{j \in \mathcal{N}_i}$ and the positions of the obstacles $\{\mathbf{p}_{k,o}\}_{k \in \mathcal{N}_i}$ within the sensing range. First, it computes the relative states of the neighboring nodes $\{\mathbf{x}_j - \mathbf{x}_i\}_{j \in \mathcal{N}_i}$ and the relative positions of the sensed obstacles $\{\mathbf{p}_{k,o} - \mathbf{p}_i\}_{k \in \mathcal{N}_i}$, and passes the latter through the message aggregation functions $\mathcal{F}_{m,a}, \mathcal{F}_{m,o}$ as

$$\sum_{j \in \mathcal{N}_i} \mathcal{F}_{m,a}(\mathbf{x}_j - \mathbf{x}_i) + \sum_{k \in \mathcal{N}_i} \mathcal{F}_{m,o}(\mathbf{p}_{k,o} - \mathbf{p}_i).$$

Then, it passes the aggregated information through the feature update function \mathcal{F}_u to generate the output as

$$\begin{aligned} & \Phi_i(\mathbf{x}_i^{(t)}, \{\mathbf{x}_j^{(t)}\}_{j \in \mathcal{N}_i}, \{\mathbf{p}_{k,o}\}_{k \in \mathcal{N}_i}, \boldsymbol{\theta}_i) \\ &= \mathcal{F}_u \left(\sum_{j \in \mathcal{N}_i} \mathcal{F}_{m,a}(\mathbf{x}_j - \mathbf{x}_i) + \sum_{k \in \mathcal{N}_i} \mathcal{F}_{m,o}(\mathbf{p}_{k,o} - \mathbf{p}_i) \right), \end{aligned} \quad (25)$$

where $\boldsymbol{\theta}_i$ are the function parameters of $\mathcal{F}_{m,a}, \mathcal{F}_{m,o}$ and \mathcal{F}_u . By sharing $\mathcal{F}_{m,a}, \mathcal{F}_{m,o}$ and \mathcal{F}_u over all nodes, we have $\boldsymbol{\theta}_1 = \dots = \boldsymbol{\theta}_N$ and thus $\Phi_1 = \dots = \Phi_N$. There are three key properties of the designed GNN:

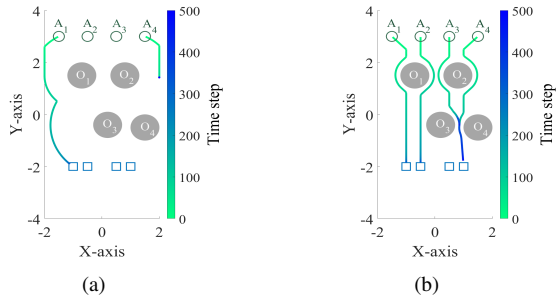


Fig. 3. (a) Robot trajectories with the minimal fixed CBF parameters (i.e., the most conservative case) selected from Figs. 2b-2c. The robots A_2 , A_3 and A_4 have overly conservative CBF constraints and the resulting QP controllers have no feasible solution. (b) Robot trajectories with the maximal fixed CBF parameters (i.e., the most aggressive case) selected from Figs. 2b-2c. The robots A_3 and A_4 have overly aggressive CBF constraints and collide in the narrow passage between the obstacles O_3 and O_4 .

(i). Decentralized execution. The resulting GNN-based policies can be executed in a decentralized manner. Specifically, the message aggregation functions $\mathcal{F}_{m,a}, \mathcal{F}_{m,o}$ require the states of the neighboring nodes and the positions of the sensed obstacles, which can be obtained through communications and sensing. The feature update function \mathcal{F}_u is a local operation that does not affect the decentralization. Therefore, each node A_i can compute its output with only local neighborhood information.

(ii). Translation invariance. The designed GNN is invariant to translations in \mathbb{R}^2 . Specifically, let $\hat{\mathbf{p}}_i = \mathbf{p}_i + \Delta$ and $\hat{\mathbf{d}}_i = \mathbf{d}_i + \Delta$ be the translated position and destination of node A_i for $i = 1, \dots, N$, where $\Delta \in \mathbb{R}^2$ is the space translation. The relative information remains the same for the translated scenario, e.g., $\hat{\mathbf{p}}_j - \hat{\mathbf{p}}_i = \mathbf{p}_j - \mathbf{p}_i$.

(iii). Permutation equivariance. The designed GNN is equivariant to permutations, i.e., the robot reordering / relabeling. Specifically, let $\Pi \in \{0, 1\}^{N \times N}$ be the permutation matrix with $\Pi\mathbf{1} = \mathbf{1}$ and $\Pi^T\mathbf{1} = \mathbf{1}$, which reorders the columns / rows of the matrix. Since all nodes share the same message aggregation and feature update functions $\mathcal{F}_{m,a}, \mathcal{F}_{m,o}$ and \mathcal{F}_u , the robot order / index has no effect on the GNN output. Therefore, the GNN applied on the permuted states $\Pi\mathbf{x}$ and the permuted graph $\Pi\mathcal{E}\Pi^T$, generates equally permuted outputs. Both translation invariance and permutation equivariance improve the sample efficiency during training, and facilitate robust transfer to unseen scenarios during testing.

V. EXPERIMENTS

In this section, we evaluate the proposed approach for multi-robot navigation. First, we conduct a proof of concept with 4 robots and 4 obstacles. Then, we show the robustness and generalization of the proposed approach to changed testing scenarios. Lastly, we consider large scenarios with more obstacles and compare performance with an exhaustive grid-search based baseline.

A. Proof of Concept

We consider an environment as shown in 2a. The robots are of radius 0.15, and are initialized randomly in the top region and tasked towards goal positions in the bottom

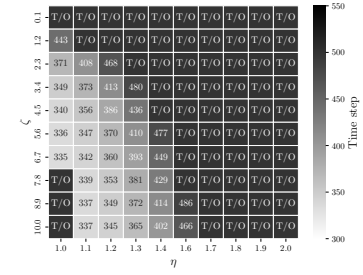


Fig. 4. Performance of grid search with ζ (vertical axis) ranging from 0.1 to 10 and η (horizontal axis) ranging from 1 to 2. The T/O stands for timeout after a threshold of 500 time steps has occurred.

region. The obstacles are of radius 0.5, which are distributed between initial and goal positions of the robots.

Implementation details. The robots are represented by positions $\{\mathbf{p}_i\}_{i=1}^N$ and velocities $\{\mathbf{v}_i\}_{i=1}^N$, and the obstacles are represented by positions $\{\mathbf{p}_{k,o}\}_{k=1}^M$. At each time step, the robot generates desired CBF parameters with a local policy based on neighborhood information, and feeds the latter into the QP controller to generate the feasible velocity towards its destination. An episode ends if all robots reach destinations or the episode times out. The sensing range, i.e., the communication radius, is 2, the maximal velocity is 0.5 per time step at each axis, the maximal time step is 500, and the time interval is 0.05. At time t , the reward is defined as

$$r_i^{(t)} = \left(\frac{\mathbf{p}_i^{(t)} - \mathbf{d}_i}{\|\mathbf{p}_i^{(t)} - \mathbf{d}_i\|_2} \cdot \frac{\mathbf{v}_i^{(t)}}{\|\mathbf{v}_i^{(t)}\|_2} \right) \|\mathbf{v}_i^{(t)}\|_2 + r_{QP}^{(t)} \quad (26)$$

where the first term rewards fast movement towards destination and the second term represents the infeasibility penalty of the QP controller. The message aggregation and feature update functions of the GNN are multi-layer perceptrons (MLPs), and the training is conducted with PPO [32].

Performance. Fig. 2a shows the robot trajectories with time-varying CBFs of the GNN-based policy. We see that the robots move smoothly from initial positions to goal positions without collision with the obstacles or each other, which validates the effectiveness of the proposed approach. Fig. 2b shows the variation of CBF parameters ζ and η of an example robot A_3 w.r.t. the other robots and obstacles, respectively. We see that (i) the values of ζ w.r.t. the other robots and obstacles remain maximal for the majority of its trajectory, which can be interpreted as relaxing the CBF constraints to generate fast velocities towards the destination, (ii), the values of ζ drop and the values of η increase between time step 100 and 150, which make the CBF constraints conservative to avoid obstacles and inter-robot collisions. I.e., robot A_3 slows its velocity to make way for robot A_4 when preparing to pass through the narrow passage between the obstacles O_3 and O_4 , and (iii), the values of ζ and η tend to be random after time step 250. This is because the robot is close to the destination and the CBF parameters play little role for navigation at that stage.

To better show the trade-off between the conservative and aggressive performance inherent in CBF parameters, we select the minimal and the maximal sets of CBF parameters from the time-varying CBF policy in Figs. 2b-2c, corre-

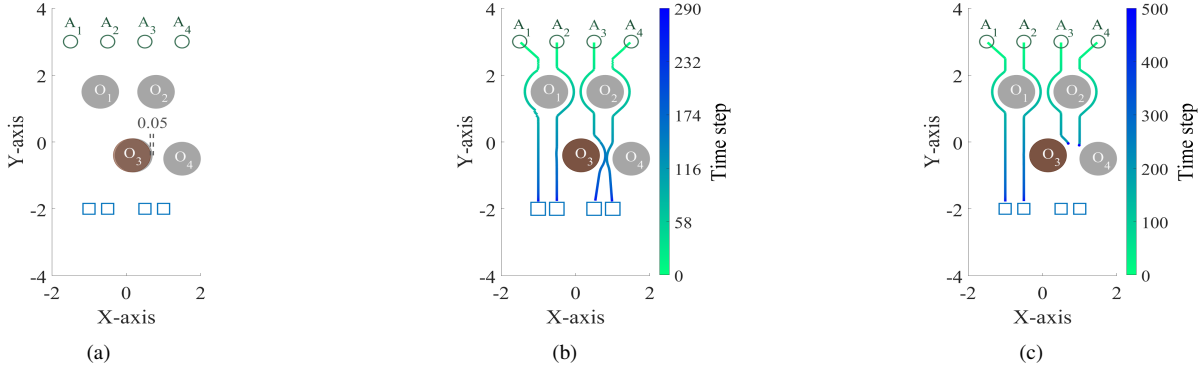


Fig. 5. (a) We modify the test-environment through a position change of obstacle O_3 from the training scenario by shifting obstacle O_3 with 0.05. (b) Robot trajectories with time-varying CBF parameters of the GNN-based policy for the new test-environment, i.e., the changed scenario. (c) Robot trajectories with fixed CBF parameters as a result of exhaustive grid-search for the new test-environment, i.e., the changed scenario. The grid-search fails the navigation tasks of the robots A_3 and A_4 in the new test-environment.

sponding to the most conservative CBF constraints in Fig. 3a and the most relaxed CBF constraints in Fig. 3b. The selected CBF parameters are fixed during the navigation procedure as in conventional CBF methods [5], [6], [15]. Fig. 3a shows how the robots A_2 , A_3 keep still and the robots A_1 , A_4 move along the environment boundary, with overly conservative trajectories, and only robot A_1 is able to reach its destination. In Fig. 3b, while all robots are aggressively steered towards their destinations, the robots A_3 and A_4 collide in the narrow passage between the obstacles O_3 and O_4 because the CBF constraints are too relaxed. These results demonstrate the importance of time-varying CBF parameters for multi-robot navigation.

B. Generalization

We evaluate the generalization capability of the proposed approach by testing the trained policy on the previously unseen environment. We consider a fixed CBF baseline tuned through exhaustive grid-search that searches CBF parameters ζ and η ranging from $[0.1, 10] \times [1.0, 2.0]$, where the selected ζ and η are fixed for all robots during navigation. We execute the proposed approach and the grid-search on the environment in Fig. 2a during training. Fig. 4 shows the result of the grid-search and the optimal CBF parameters are set to $\zeta = 6.7$, $\eta = 1.0$. While exhaustively traversing all combinations, the grid search is inefficient with the majority of the search being infeasible. We change the environment during testing, as depicted in Fig. 5a, which slightly shifts obstacle O_3 with 0.05.

Figs. 5b-5c display the performance of the GNN-based policy and the grid-search on the changed environment. We see that the proposed approach successfully steers all robots towards goal positions, yielding good transfer during testing. However, the grid search cannot complete the navigation tasks of the robots A_3 and A_4 , i.e., the robots A_3 and A_4 collide in the changed environment. We remark that the grid search fails with a small change (i.e., 0.05 left shift) of the environment, which shows the vulnerability of fixed CBFs and highlights the importance of time-varying CBFs proposed by our approach.

C. Large Scenario

We now conduct performance comparison in a large environment with 8 obstacles, where the maximal time step

is 750. We perform the proposed approach and the grid-search in the environment as shown in Fig. 6a, and test them by randomly shifting initial, goal and obstacle positions. We measure the performance by two metrics: Success weighted by Path Length (SPL) [33] and the percentage to the maximal speed (PCTSpeed). The former metric combines navigation success rate with path length overhead, while the latter metric represents the ratio of the average speed to the maximal one.

Fig. 6b shows the results average over 20 random trials. We see that the proposed approach outperforms the grid search in both metrics, with higher expected performance and lower standard deviations. This demonstrates the effectiveness of the proposed approach in large scenarios and corroborates its robustness to environment changes, as shown in Sec. V-B.

Moreover, it is note-worthy that there exist environment scenarios where there is no solution for the grid-search with fixed CBF parameters. Specifically, consider the environment setting in Fig. 6c. The proposed approach solves navigation tasks of all robots successfully without collision – see Fig. 6c. However, our grid-search fails to find any feasible solution. This result further shows the superiority of the environment-aware CBFs with the proposed approach to the fixed CBFs with the grid-search.

VI. CONCLUSION

This paper proposed environment-aware control barrier functions (CBFs) for multi-robot navigation. We formulated the problem of multi-robot navigation as a quadratic programming problem with state convergence w.r.t. control Lyapunov functions and safety constraints w.r.t. CBFs, and proposed the novel problem of CBF optimization that tunes CBF constraints based the dynamic environment in a real-time and decentralized manner. Our overarching goal was to pursue a trade-off between conservativeness and aggressiveness of robots' behaviors from CBF constraints to improve the navigation performance whilst ensuring safety. We solved this problem by leveraging model-free reinforcement learning with a GNN-based architecture. The former overcomes the challenge of explicitly modeling the relationship between CBF parameters and navigation performance, and the latter allows each robot to adjust its CBF parameters locally with perceived neighborhood information during navigation. We

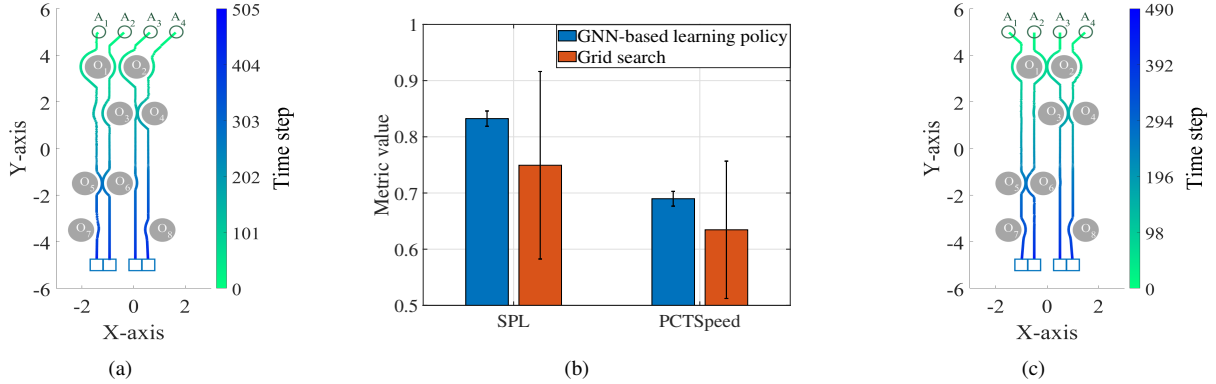


Fig. 6. (a) Robot trajectories with time-varying CBF parameters of GNN-based policy in an environment with 4 robots and 8 obstacles. (b) Performance comparison between GNN-based policy and grid-search. The results are averaged over 20 random trials and the error bar shows the std. dev. (c) Robot trajectories with time-varying CBF parameters of GNN-based policy in the environment setting where there is no feasible solution resulting from the grid-search.

evaluated the proposed approach by comparing with exhaustive grid-search in a variety of environment settings. The results show the superiority of environment-aware CBFs with improved robustness in dynamic environments with robot movement and obstacle reconfigurations. In future work, we will extend our work on non-linear systems with a higher relative degree. Furthermore, we will validate our framework on real hardware and perform navigation with rich mission specifications.

REFERENCES

- [1] J. Ota, "Multi-agent robot systems as distributed autonomous systems," *Advanced Engineering Informatics*, vol. 20, no. 1, pp. 59–70, 2006.
- [2] Y. Wang, E. Garcia, D. Casbeer, and F. Zhang, "Cooperative control of multi-agent systems: Theory and applications," 2017.
- [3] A. Oroojlooy and D. Hajinezhad, "A review of cooperative multi-agent deep reinforcement learning," *Applied Intelligence*, pp. 1–46, 2022.
- [4] A. D. Ames, J. W. Grizzle, and P. Tabuada, "Control barrier function based quadratic programs with application to adaptive cruise control," in *IEEE Conference on Decision and Control (CDC)*, 2014.
- [5] Q. Nguyen and K. Sreenath, "Exponential control barrier functions for enforcing high relative-degree safety-critical constraints," in *IEEE American Control Conference (ACC)*, 2016.
- [6] S.-C. Hsu, X. Xu, and A. D. Ames, "Control barrier function based quadratic programs with application to bipedal robotic walking," in *IEEE American Control Conference (ACC)*, 2015.
- [7] U. Borrman, L. Wang, A. D. Ames, and M. Egerstedt, "Control barrier certificates for safe swarm behavior," *IFAC-PapersOnLine*, vol. 48, no. 27, pp. 68–73, 2015.
- [8] Z. Gao and A. Prorok, "Environment optimization for multi-agent navigation," *arXiv preprint arXiv:2209.11279*, 2022.
- [9] Q. Li, F. Gama, A. Ribeiro, and A. Prorok, "Graph neural networks for decentralized multi-robot path planning," in *IEEE/RSJ International Conference on Intelligent Robots and Systems (IROS)*, 2020.
- [10] E. Tolstaya, F. Gama, J. Paulos, G. Pappas, V. Kumar, and A. Ribeiro, "Learning decentralized controllers for robot swarms with graph neural networks," in *Conference on Robot Learning (CoRL)*, 2020.
- [11] Z. Gao, F. Gama, and A. Ribeiro, "Wide and deep graph neural network with distributed online learning," *IEEE Transactions on Signal Processing*, vol. 70, pp. 3862–3877, 2022.
- [12] L. Lindemann and D. V. Dimarogonas, "Control barrier functions for multi-agent systems under conflicting local signal temporal logic tasks," *IEEE Control Systems Letters*, vol. 3, no. 3, pp. 757–762, 2019.
- [13] X. Tan and D. V. Dimarogonas, "Distributed implementation of control barrier functions for multi-agent systems," *IEEE Control Systems Letters*, vol. 6, pp. 1879–1884, 2021.
- [14] O. Özkahraman and P. Ogren, "Combining control barrier functions and behavior trees for multi-agent underwater coverage missions," in *IEEE Conference on Decision and Control (CDC)*, 2020.
- [15] M. Srinivasan, S. Coogan, and M. Egerstedt, "Control of multi-agent systems with finite time control barrier certificates and temporal logic," in *IEEE Conference on Decision and Control (CDC)*, 2018.
- [16] Z. Qin, K. Zhang, Y. Chen, J. Chen, and C. Fan, "Learning safe multi-agent control with decentralized neural barrier certificates," *arXiv preprint arXiv:2101.05436*, 2021.
- [17] M. Ahmadi, A. Singletary, J. W. Burdick, and A. D. Ames, "Safe policy synthesis in multi-agent pomdps via discrete-time barrier functions," in *IEEE Conference on Decision and Control (CDC)*, 2019.
- [18] C. Yu, H. Yu, and S. Gao, "Learning control admissibility models with graph neural networks for multi-agent navigation," *arXiv preprint arXiv:2210.09378*, 2022.
- [19] C. Folkestad, Y. Chen, A. D. Ames, and J. W. Burdick, "Data-driven safety-critical control: Synthesizing control barrier functions with koopman operators," *IEEE Control Systems Letters*, vol. 5, no. 6, pp. 2012–2017, 2021.
- [20] K. Xu, W. Xiao, and C. G. Cassandras, "Feasibility guaranteed traffic merging control using control barrier functions," in *IEEE American Control Conference (ACC)*, 2022.
- [21] J. Zeng, B. Zhang, and K. Sreenath, "Safety-critical model predictive control with discrete-time control barrier function," in *IEEE American Control Conference (ACC)*, 2021.
- [22] J. Zeng, Z. Li, and K. Sreenath, "Enhancing feasibility and safety of nonlinear model predictive control with discrete-time control barrier functions," in *IEEE Conference on Decision and Control (CDC)*, 2021.
- [23] J. Breeden, K. Garg, and D. Panagou, "Control barrier functions in sampled-data systems," *IEEE Control Systems Letters*, vol. 6, pp. 367–372, 2021.
- [24] W. Xiao, C. A. Belta, and C. G. Cassandras, "Feasibility-guided learning for constrained optimal control problems," in *IEEE Conference on Decision and Control (CDC)*, 2020.
- [25] A. D. Ames, K. Galloway, K. Sreenath, and J. W. Grizzle, "Rapidly exponentially stabilizing control lyapunov functions and hybrid zero dynamics," *IEEE Transactions on Automatic Control*, vol. 59, no. 4, pp. 876–891, 2014.
- [26] H. K. Khalil, "Nonlinear systems third edition," *Patience Hall*, vol. 115, 2002.
- [27] W. Xiao and C. Belta, "Control barrier functions for systems with high relative degree," in *IEEE Conference on Decision and Control (CDC)*, 2019.
- [28] X. Xu, P. Tabuada, J. W. Grizzle, and A. D. Ames, "Robustness of control barrier functions for safety critical control," *IFAC-PapersOnLine*, vol. 48, no. 27, pp. 54–61, 2015.
- [29] F. Scarselli, M. Gori, A. C. Tsoi, M. Hagenbuchner, and G. Monfardini, "The graph neural network model," *IEEE Transactions on Neural Networks*, vol. 20, no. 1, pp. 61–80, 2009.
- [30] P. Veličković, G. Cucurull, A. Casanova, A. Romero, P. Liò, and Y. Bengio, "Graph attention networks," in *International Conference on Learning Representations (ICML)*, 2018.
- [31] Z. Gao, E. Isufi, and A. Ribeiro, "Stochastic graph neural networks," *IEEE Transactions on Signal Processing*, vol. 69, pp. 4428–4443, 2021.
- [32] J. Schulman, F. Wolski, P. Dhariwal, A. Radford, and O. Klimov, "Proximal policy optimization algorithms," *arXiv preprint arXiv:1707.06347*, 2017.
- [33] P. Anderson, A. Chang, D. S. Chaplot, A. Dosovitskiy, S. Gupta, V. Koltun, J. Kosecka, J. Malik, R. Mottaghi, M. Savva *et al.*, "On evaluation of embodied navigation agents," *arXiv preprint arXiv:1807.06757*, 2018.